L-6: *Late-News Paper:* Achromatic Diffraction Using Reactive Mesogen Polarization Gratings

***Chulwoo Oh and Michael J. Escuti*[1]**

Dept. of Electrical and Computer Engineering, North Carolina State University, Raleigh, NC, USA

Abstract

We propose and experimentally demonstrate an achromatic polarization grating, with ~100% diffraction efficiency over nearly the entire visible spectral range. This five-fold enhancement (~34.3% versus ~6.8%) is produced by two chiral liquid crystal layers with modest twist angle and opposite twist sense. Finite-difference time-domain (FDTD) simulations support the experimental phenomena.

1. Introduction

Our objective is to design diffractive optical elements with unprecedented control of the direction and polarization state of transmitted light over a broad spectral range. Elements such as these have high potential benefit to display applications, including efficient outcoupling from backlights, polarization-independent pixel designs, and light recycling. To this end, we employ a novel anisotropic periodic structure, known as a polarization grating (PG) [1]. PGs can manifest unique diffraction properties – only three possible orders (0 and ±1) with special polarizations and up to 100% efficiency – and supports a wide range of applications. However, the spectral range over which the conventional PG ideally diffracts with high efficiency is at best ~7% of the center wavelength. Here we report our development of an achromatic PG which shows a five-fold increase in this bandwidth, and which diffracts with ~100% efficiency even with broadband illumination (e.g. white light).

Since PGs were introduced as elemental polarization holograms [1], many researchers have studied their diffraction properties and utility. For example, early applications of PGs included polarization measurement [2] and spectropolarimetry [3,4]. Nematic liquid crystals (LCs) were recently discovered to advantageously create a continuous-texture PGs with linear birefringence [5,6]. This approach was subsequently used to create defect-free, switchable PGs [7] with ideal diffraction properties and very low scattering when carefully reduced to experiment. Since these were highly-efficient, they could be configured as a polarization-independent modulator. A prototype of a Schlieren projection system based on an LC polarization grating (LCPG) microdisplay was demonstrated at the 2006 SID Symposium [8].

The conventional ("Circular"-type) PG is composed of a spatially-variant uniaxial birefringence (i.e. $\mathbf{n}(x)=[\cos(\pi x/\Lambda), \sin(\pi x/\Lambda), 0]$), as shown in Fig. 1(a) and 1(b). The ideal diffraction efficiency at normal incidence can be derived with Jones calculus [3]:

$$\eta_0 = \cos^2\left(\frac{\pi\Delta n d}{\lambda}\right) \quad \text{and} \quad \eta_{\pm 1} = \frac{1}{2}\left[1 \mp S_3'\right]\sin^2\left(\frac{\pi\Delta n d}{\lambda}\right) \qquad (1)$$

where η_m is the diffraction efficiency of the m^{th}-order, λ is the vacuum wavelength of incident light, Δn is the linear birefringence, d is the grating thickness, and $S_3' = S_3/S_0$ is the normalized Strokes parameter corresponding to ellipticity of the incident light. Only three orders (0 and ±1) are present, and the first orders possess orthogonal circular polarizations (left- and right-hand). Note that the diffraction behavior of PGs depends modestly on the wavelength (through $\Delta n d/\lambda$ in Eqs. (1)).

Here, we propose and demonstrate the achromatic performance of the PG based on a two-layer twisted structure as shown in Fig. 1(c) and 1(d), performing nearly 100% efficiency across a wide spectral width (34.3%, a factor of five increase). Achromatic operation by retardation compensation of double-layered super-twisted nematic (STN) LC cells is well known in display circles [9]. We have discovered that a similar achromacity of PG diffraction can be achieved by combining two twisted PGs with opposite twist sense.

Key design parameters for broadband diffraction of twisted PGs are thickness d and twist angle θ_{twist} of each layer. To demonstrate the optimal conditions for these parameters, we applied the finite-difference time-domain (FDTD) method using an open-source software package *WOLFSIM*, developed at NCSU especially for periodic anisotropic media [10,11]. This paper also presents preliminary experimental results of the achromatic PG formed as a polymer film of reactive mesogens (RMs), also

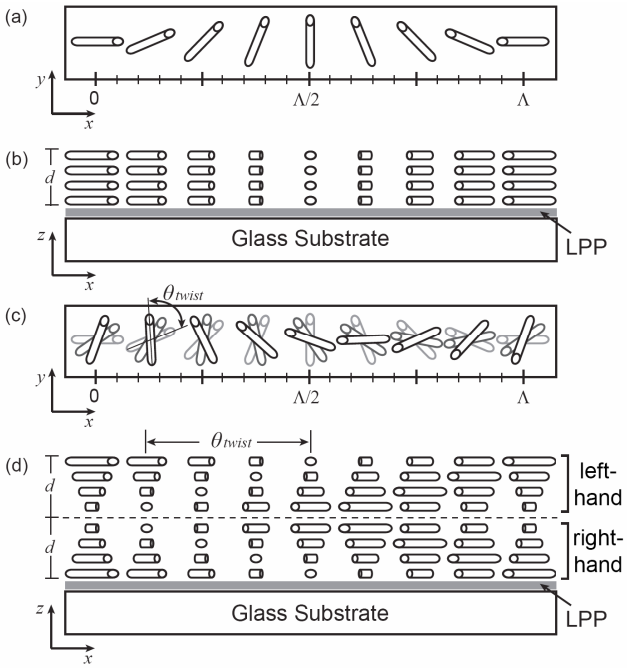

Figure 1: Polarization Gratings (PG) – Basic geometry of a conventional PG, (a) top view & (b) side view; Achromatic PG with two chiral layers (opposite twist sense), (c) top view & (d) side view. The double-layered twist structure leads to efficient broadband diffraction by retardation compensation.

[1] Preferred email contact: mjescuti@ncsu.edu

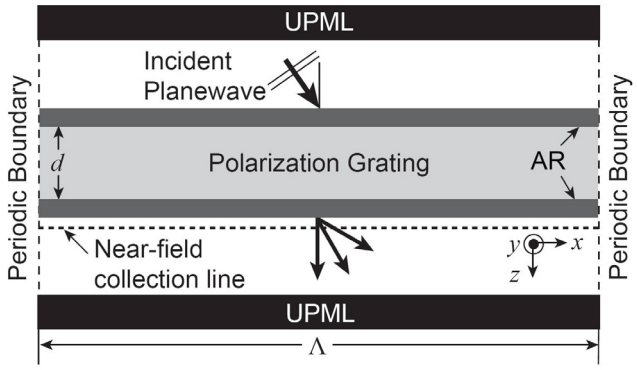

Figure 2: Layout of the 2D+ FDTD simulation space.

known as polymerizable liquid crystals, using polarization holography and photo-alignment techniques.

2. Numerical Results

We modeled the PG with *WOLFSIM* [10,11], which easily accepts space-variant anisotropic dielectric properties. Fig. 2 shows the basic geometry of the FDTD simulation space for our analysis. Note that we apply gradient-index anti-reflection coatings at both air-PG interfaces to minimize Fresnel losses. Periodic boundaries and the perfectly matched layer boundaries are employed to terminate the simulation space, and minimize simulation time. The input is a Gaussian-pulsed planewave (a wideband source) with vertical-linear polarization placed just before the grating structure, and the output diffraction efficiencies are calculated from the electric field at a line immediately after the grating. A near-to-far optical transformation and a temporal Fourier transform are used to analyze spectral diffraction properties in the far-field [10].

We define the spectral range $\Delta\lambda$ (units of wavelength) for high PG efficiency as the range of wavelengths over which the total first-order diffraction $\Sigma\eta_{\pm1}$ is $\geq$ 99.5%. The normalized bandwidth $\Delta\lambda/\lambda_{center}$ (units of %) is defined as the ratio of the spectral range to its center wavelength λ_{center}.

We begin by simulating diffraction properties of the PG with only one twist (data is the same for right- and left-handedness). Fig. 3 shows a sum of the first-order efficiency ($\Sigma\eta_{\pm1}$) versus normalized retardation ($\Delta nd/\lambda$) for different twist angles (θ_{twist}) from 0° to 90°. The maximum high-efficiency bandwidth occurs in the conventional PG case (θ_{twist} = 0°), and results in $\Delta\lambda/\lambda_{center}$ = 6.8%. Since the condition for adiabatic-following (also known as waveguding) is not met except for very small twist angles, a marked degradation in efficiency results with increasing twist angle. Nevertheless, only the 0 and ±1-orders are present in the output and the first-order polarizations become increasingly elliptical (as opposed to circular).

However, high diffraction efficiency (~100%) can be recovered by stacking two twisted PGs with opposite twist sense. Since the optical properties of both layers are identical except the sign of twist, the second layer compensates the polarization effect of the first twisted structure. We therefore qualitatively describe the achromatic effect as localized retardation compensation.

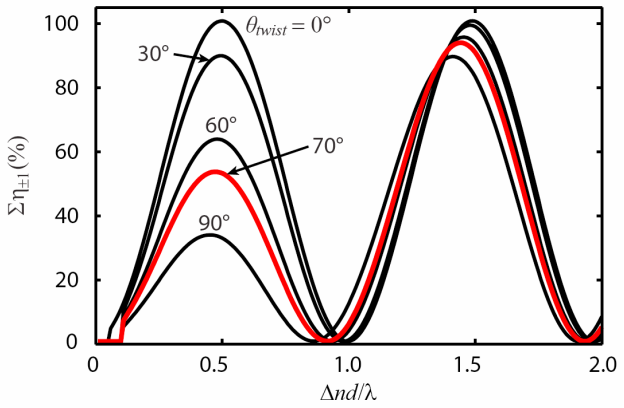

Figure 3: Simulated diffraction spectra of the conventional PG for different twist angles. (Λ=20λ_0 and d=2.5λ_0)

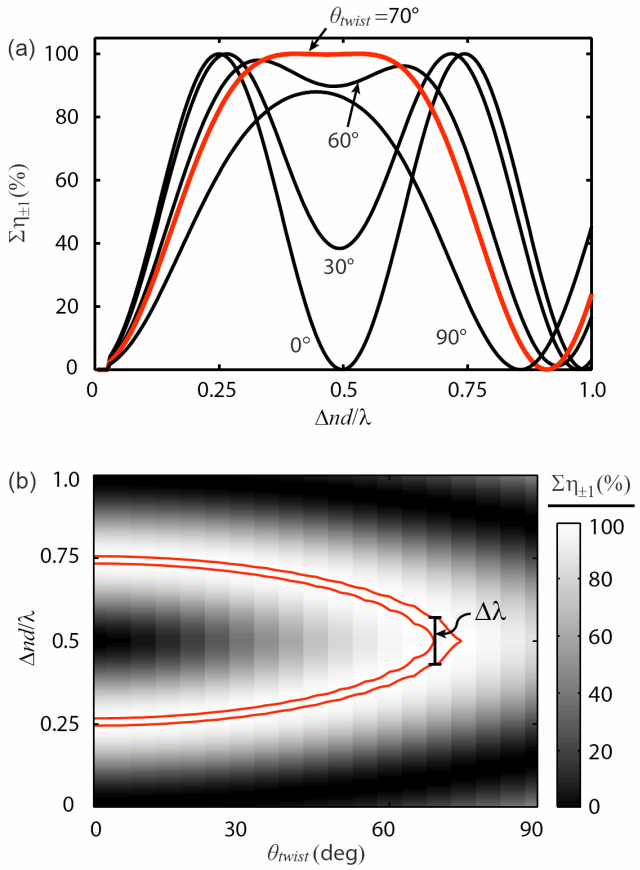

Figure 4: Simulated results of PGs composed of two twisted layers and opposite twist sense: (a) Diffraction spectra for different twist angles; (b) Spectral range for high efficiency (≥99.5%, enclosed area). Gray scale levels depict simulated diffraction efficiency and the bandwidth $\Delta\lambda/\lambda_{center}$ is maximized at the region shown. Note that d is the thickness of each grating layer and the final grating thickness is 2d. (Λ=20λ_0 and d=2.5λ_0)

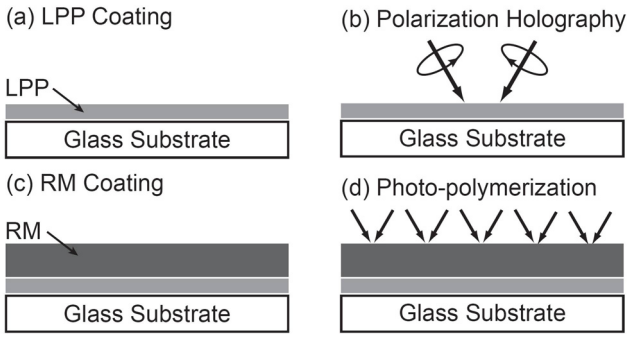

Figure 5: Fabrication steps of reactive mesogen PGs using polarization holography and photo-alignment techniques.

To find the optimum θ_{twist}, we ran a series of simulations with varying the twist angle from 0° to 90°. Fig. 4(a) shows the first order efficiency ($\Sigma\eta_{\pm1}$) as a function of normalized retardation ($\Delta nd/\lambda$) for different values of θ_{twist}. We find that the maximum bandwidth $\Delta\lambda/\lambda_{max}$ = 34.3% can be achieved when θ_{twist} = 70° as shown in Fig. 4(b). Note that this is a five-fold enhancement in the maximum diffraction bandwidth as compared with the conventional PG. Since the diffraction bandwidth is highly sensitive to the twist angle, a careful control of θ_{twist} is required to get the best performance of the bandwidth

3. Experimental Results

We also experimentally demonstrated the achromatic PG formed as a reactive mesogen (RM) film by polarization holography and photo-alignment techniques [5,7]. We have recently [3] fabricated defect-free RM PGs (conventional) with ultra-high efficiency and low scattering by materials and processing optimization. As shown in Fig. 5, fabrication of reactive mesogen PGs proceeds with following four basic steps: first, a thin layer of photo-alignment material is coated on a glass substrate (Fig. 5(a)); second, the substrate is exposed with two coherent beams from a laser with orthogonal circular polarizations at a small angle, leading to polarization interference with a constant intensity (Fig. 5(b)); third, the RM mixture is coated on the photo-alignment layer and made to be align according to the surface pattern (Fig. 5(c)); finally, the RM layer is photo-polymerized with a blanket ultraviolet exposure to permanently fix the large structured optical anisotropy (Fig. 5(d)).

We use this basic fabrication also for the achromatic PG. In particular, we utilized a linear-photopolymerizable polymer (LPP) [12] ROP-103 (Rolic) as a photo-alignment material. A HeCd laser (325 nm) with orthogonal circular polarized beams was used to expose a surface alignment pattern with a period of Λ=8.5μm onto the LPP layer. After LPP exposure, RM films were deposited on the LPP-coated substrate by spin-coating. The first RM layer was a mixture composed of RMS03-001 (Merck, Δn ~ 0.159 at 589 nm) with small amount (0.25%) of chiral dopant CB15 (Merck, right-handedness), chosen so that the RM layer reached the half-wave thickness ($d=\lambda/2\Delta n$) and θ_{twist}=70°. The second RM layer was deposited directly on top of the first, and was composed of RMS03-001 doped with a small amount (0.34%) of a different chiral agent, ZLI-811 (Merk, left-handedness), subject to the same thickness and twist condition.

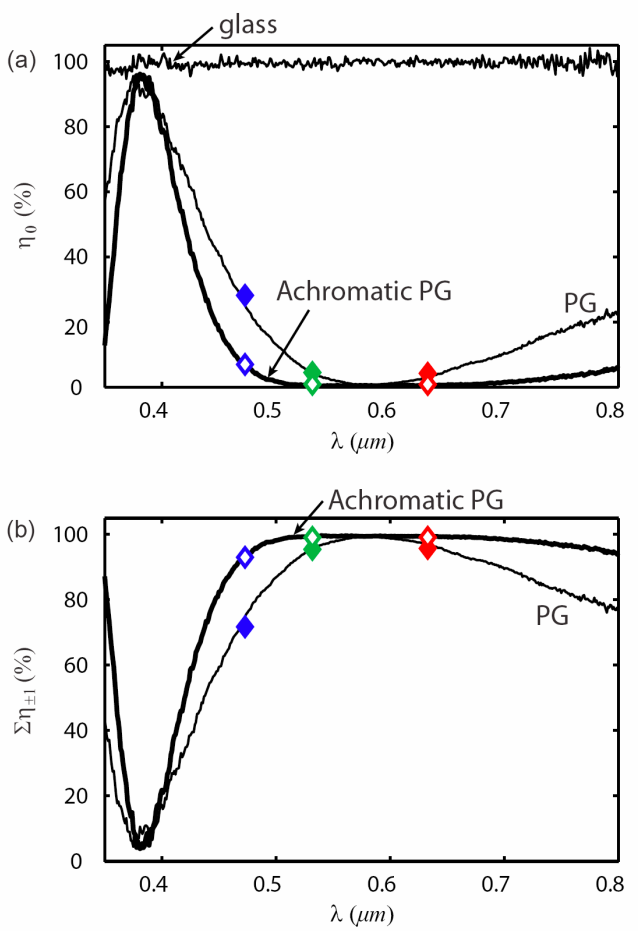

Figure 6: Experimental results from the achromatic PG (Λ=8.5μm) as implemented with reactive mesogens: (a) the 0-order efficiency spectra; (b) estimated first-order efficiency spectra, calculated from the 0-order ($\Sigma\eta_{\pm1} \approx 1-\eta_0$). A clean glass slide is shown as reference in part (a). Diffraction spectra (experimentally measured) of a conventional RMPG are shown for comparison. Exact efficiencies (diamonds) at three wavelengths were measured with red (633nm), green (532nm), and blue (473nm) lasers for both the achromatic PG (white face-color) and the conventional PG (colored-face).

Note that the final grating thickness was ~2d, because two layers were stacked (each with the half-wave thickness).

Fig. 5(a) shows the 0-order efficiency spectra of both samples of the normal PG and the achromatic PG, measured with a spectrophotometer. Note the measured transmittance of a clean glass slide (~100%) measured under the identical conditions to the PGs. The spectra of the estimated diffraction efficiency ($\sum\eta_{\pm1} \approx 1 - \eta_0$) is plotted in Fig. 5(b). As expected from FDTD simulation results, a noticeable improvement in the diffraction bandwidth is found. Exact efficiencies at three lasers wavelengths were also measured at red (633 nm), green (532 nm), and blue (473 nm) wavelengths, which conclusively confirm the estimated efficiencies in Fig. 5(b). Note that the diffraction efficiency is defined as $\eta_m = I_m / I_{REF}$, where I_m is the measured

intensity of the m^{th} transmitted diffracted order, and where I_{REF} is a reference transmission intensity for a glass substrate. Note that we roughly measured the incoherent scattering as 2% or less above 400 nm, by comparing the diffracted spectra to the clean glass slide.

6. Discussion

We highlight that the achromatic PG retains all the unique diffraction properties of the conventional PG: only three diffracted orders (0, ±1), orthogonal circular polarizations of the first orders, and highly polarization-sensitive first orders. Incident circular polarization can produce ~100% efficiency into one of the first orders and linear incident polarization or unpolarized input can give ~50% efficiency into each of the first orders. Compared to other LC gratings (i.e. polymer-wall LC gratings [13] and HPDLC gratings [14,15]), PGs promise comparable or higher experimental diffraction efficiencies, and lower incoherent scattering. In effect, the achromatic PG offers the high efficiencies of thick (Bragg) gratings over a nearly the entire range of visible light. When used as an optical element of displays, the achromatic PG may be integrated with other optical components and can make the display more compact and efficient. We also note that a similar achromatic design of the PG can be implemented as a switchable LC grating for modulator applications, by allowing one of the grating twists to be implemented as a non-reactive nematic and by placing the entire structure between substrates with electrodes.

5. Conclusions

The achromatic PG, which achieves ultra-high efficiency over a broad spectral range, offers a wide range of potential applications in display technologies with benefits of efficient control of light by its unique diffraction behavior. Here, we optimized the grating parameters (thickness and twist angle) for maximum bandwidth using FDTD simulations, and experimentally realized a high-quality achromatic PG using reactive mesogens with improved bandwidth (almost over the entire visible range) for high diffraction efficiency and low scattering.

6. Acknowledgements

The authors gratefully acknowledge support from the National Science Foundation (grant ECCS-0621906).

7. References

[1] L. Nikolova and T. Todorov, “Diffraction efficiency and selectivity of polarization holographic recording,” *Optica Acta*, Vol. **31**, pp. 579-588, 1984.

[2] F. Gori, “Measuring Stokes parameters by means of a polarization grating,” *Opt. Lett.*, Vol. **24**, pp. 584-586, 1999.

[3] M. J. Escuti, C. Oh, C Sanchez, C W M Bastiaansen, and D J Broer, “Simplified Spectropolarimetry Using Reactive Mesogen Polarization Gratings,” *Proc. SPIE*, Vol. **6302**, pp. 630207, 2006.

[4] C. Provenzano, G. Cipparrone, and A. Mazzulla, “Photopolarimeter based on two gratings recorded in thin organic films,” *Appl. Opt.*, Vol. **45**, pp. 3929-3934, 2006.

[5] G. P. Crawford, J. N. Eakin, M. D. Radcliffe, A. Callan-Jones, and R. A. Pelcovits, “Liquid-crystal diffraction gratings using polarization holography alignment techniques,” *J. Appl. Phys.*, Vol. **98**, pp. 123102, 2005.

[6] H. Sarkissian, S. V. Serak, N. V. Tabiryan, L. B. Glebov, V. Rotar, and B. Y. Zeldovich, “Polarization-controlled switching between diffraction orders in transverse-periodically aligned nematic liquid crystals,” *Opt. Lett.*, Vol. **31**, pp. 2248-2250, 2006.

[7] M. J. Escuti and W. M. Jones, “Polarization independent switching with high contrast from a liquid crystal polarization grating,” *SID Symp. Digest*, Vol. **37**, pp. 1443-1446, 2006.

[8] W M Jones, B L Conover, and M J Escuti, “Evaluation of projection schemes for the liquid crystal polarization grating operating on unpolarized light,” *SID Symp. Digest*, Vol. **37**, pp. 1015-1018, 2006.

[9] T. Scheffer and J. Nehring, “Super-twisted nematic (STN) liquid crystal displays,” *Annu. Rev. Mater. Sci.*, Vol. **27**, pp. 555-583, 1997.

[10] C. Oh and M. J. Escuti, “Time-domain analysis of periodic anisotropic media at oblique incidence: an efficient FDTD implementation,” *Opt. Express*, Vol. **14**, pp. 11870-11884, 2006.

[11] http://www.ece.ncsu.edu/oleg/wolfsim.html

[12] M. Schadt, H. Seiberle, and A. Schuster, “Optical patterning of multi-domain liquid crystal displays with wide viewing angles," *Nature*, Vol. **381**, pp. 212-215, 1996.

[13] Y. Zhang, B. Wang, P. J. Bos, J. Colegrove, and D. B. Chung, “High-efficiency, liquid-crystal-based, controllable diffraction grating,” *J. Opt. Soc. Am. A*, Vol. **22**, pp. 2510-2515, 2005.

[14] T. J. Bunning, L. V. Nataranjan, V. P. Tondiglia, and R. L. Sutherland, “Holograpic Polymer-Dispersed Liquid Crystals (H-PDLCs)," *Annu. Rev. Mater. Sci.*, Vol. **30**, pp. 83-115, 2000.

[15] G. Crawford, “Electrically switchable bragg gratings," *Opt. Photonics News*, Vol. **14**, pp. 54-59, 2003.